

The impact of void-finding algorithms on galaxy classification

FATIMA ZAIDOUNI,^{1,*} DAHLIA VEYRAT,¹ KELLY A. DOUGLASS,¹ AND SEGEV BENZVI¹

¹*Department of Physics and Astronomy, University of Rochester, Rochester, NY USA 14627*

ABSTRACT

We explore how the definition of a void influences the conclusions drawn about the impact of the void environment on galactic properties using two void-finding algorithms in the Void Analysis Software Toolkit: V^2 , a Python implementation of ZOBOV, and `VoidFinder`, an algorithm which grows and merges spherical void regions. Using the Sloan Digital Sky Survey Data Release 7, we find that galaxies found in `VoidFinder` voids tend to be bluer, fainter, and have higher (specific) star formation rates than galaxies in denser regions. Conversely, galaxies found in V^2 voids show no significant differences when compared to galaxies in denser regions, inconsistent with the large-scale environmental effects on galaxy properties expected from both simulations and previous observations. These results align with previous simulation results that show V^2 -identified voids “leaking” into the dense walls between voids because their boundaries extend up to the density maxima in the walls. As a result, when using ZOBOV-based void finders, galaxies likely to be part of wall regions are instead classified as void galaxies, a misclassification that can be critical to our understanding of galaxy evolution.

1. INTRODUCTION

The large-scale structure of the universe observed in galaxy redshift surveys exhibits a cosmic web-like structure (Bond et al. 1996) comprising voids, or vast underdense regions tens of megaparsecs across, that are bordered by filaments of galaxies that flow into large galaxy clusters (de Lapparent et al. 1986). Because of the low matter density within voids, their gravitational evolution remains in the linear regime (Sutter et al. 2012a), and the few galaxies found in voids evolve relatively free of interactions with other galaxies.

Void regions provide unique laboratories for studying both cosmology and galaxy physics. Because their evolution is partly shaped by the expansion of the universe (e.g., Lavaux & Wandelt 2012; Pisani et al. 2015; Sahlén 2019), voids are also useful for studying dark energy and provide precision constraints on cosmological models via the Alcock-Paczyński test (e.g., Lavaux & Wandelt 2012; Sutter et al. 2012b, 2014; Hamaus et al. 2016; Mao et al. 2017; Nadathur et al. 2019; Hamaus et al. 2020), as well as in neutrino studies and models of galaxy formation (Peebles 2001; Constantin et al. 2008; Sahlén

2019). In addition, voids are used in measurements of baryon acoustic oscillations via void-galaxy correlation functions (Nadathur et al. 2019; Zhao et al. 2020, 2022). Due to the extreme low density of void interiors, void galaxies rarely interact with other objects, in contrast to galaxies found in denser regions. As a result, they provide relatively undisturbed environments for studying galactic evolution.

While voids do have some universal properties, such as an underdense center ($\lesssim 5\%$ of the mean galaxy density) and a steep density gradient at their boundary (Colberg et al. 2008), the definition of what is a void is rather vague. In part, this is because void morphologies and densities exhibit significant variability. Due to the ambiguity, a number of different void finding algorithms exist to identify underdense regions.

When making conclusions based on different void catalogs, care must be taken to untangle physical effects from the details of how voids are defined. The Aspen-Amsterdam void finder comparison project (Colberg et al. 2008) performed a preliminary comparison between 13 void-finding algorithms, examining the distributions of the different algorithms’ void properties. A recent comparison of the void-finding algorithms in the Void Analysis Software Toolkit (VAST; Douglass et al. 2022) by Veyrat et al. (2023) on their ability to recover regions of the large-scale structure whose dynamics match those expected for voids found that the different algorithms do identify different dynamical regions of

Corresponding author: Kelly A. Douglass
kellyadouglass@rochester.edu

* Now at Department of Physics, Massachusetts Institute of Technology, Cambridge, MA 02139

the universe. However, the impact of the choice of void-finding algorithms on either cosmology or galaxy science has not been systematically studied. [Muldrew et al. \(2012\)](#) used mock galaxy catalogs to study how various definitions of the large-scale environment change the inferred effect of the environment on galaxy evolution. In this work, we focus on the impact of the void-finding algorithms on inferred galaxy properties by comparing the properties of the galaxies inside voids defined by different algorithms, but it does not focus on void definitions or void algorithms. This study allows us to understand how conclusions about the effects of the void environment depend on the choice of void-finding algorithm.

2. EXPECTED GALAXY EVOLUTION IN VOIDS

N-body simulations and semi-analytic models of Λ CDM cosmology predict that void galaxies are retarded in their star formation relative to galaxies in denser regions ([Cen 2011](#)). Numerous studies have been conducted to test this with observations; investigating the influence of the void environment on the galactic mass function (e.g., [Hoyle et al. 2005](#); [Croton et al. 2005](#); [Moorman et al. 2015](#)), on galaxy photometry (e.g., [Grogin & Geller 2000](#); [Rojas et al. 2004, 2005](#); [Patiri et al. 2006](#); [Park et al. 2007](#); [von Benda-Beckmann & Müller 2008](#); [Hoyle et al. 2012](#)), on the star formation rate (e.g., [Rojas et al. 2005](#); [Moorman et al. 2016](#); [Beygu et al. 2016](#)), and on chemical composition (e.g., [Kreckel et al. 2012](#); [Douglass & Vogeley 2017](#)). The vast majority of these observational studies confirm that galaxies in voids are fainter and bluer than galaxies in denser regions. This is likely a result of the retention of gas by void galaxies as they evolve in an environment with fewer interactions such as mergers, tidal stripping, ram-pressure stripping, etc., compared to galaxies in denser regions ([Cen 2011](#)).

We therefore expect void galaxies to be fainter, bluer, to have lower mass, and to have higher (specific) star formation rates regardless of the void-finding method used in the analysis. We test this by comparing the properties of void galaxies as classified using two popular void-finding algorithms. To achieve high statistical significance, we use a large sample of galaxies from the Sloan Digital Sky Survey Data Release 7 (SDSS DR7, [Abazajian et al. 2009](#)), which to our knowledge is the largest galaxy sample used to study properties of void galaxies to date. The comparisons shed light on the impact of different void-finding algorithms in galactic classification.

3. GALAXY CATALOG: SDSS DR7

SDSS DR7 ([Abazajian et al. 2009](#)) is the final public data release from SDSS-II and was designed to collect

spectra of a magnitude-complete galaxy sample, observing everything brighter than a Petrosian r -band magnitude $m_r < 17.77$ ([Strauss et al. 2002](#)). This final catalog includes 11,663 deg^2 of imaging data and five-band photometry for 357 million objects ([Lupton et al. 2001](#)). It also has complete spectroscopy with a resolution $\lambda/\Delta\lambda \sim 1800$ in the observed wavelength range 3800Å–9200Å ([Blanton et al. 2003](#)) covering a contiguous 9380 deg^2 of the Northern Galactic Cap. In total, the SDSS DR7 spectroscopic sample contains 1.6 million spectra including 930,000 galaxies, 120,000 quasars, and 460,000 stars.

We use SDSS DR7 as reprocessed and presented in the NASA-Sloan Atlas¹ (NSA, version 1.0.1), a catalog of images and parameters derived from the SDSS imaging ([Blanton et al. 2011](#)). The NSA provides K -corrected absolute magnitudes, colors, and stellar masses. Star formation rates and specific star formation rates are taken from the MPA-JHU value-added galaxy catalog² based on the method described in [Brinchmann et al. \(2004\)](#). We assume a flat Λ CDM cosmology with $\Omega_M = 0.315$ and $H_0 = 100h \text{ km s}^{-1} \text{ Mpc}^{-1}$.

4. THE VOID ANALYSIS SOFTWARE TOOLKIT

We use the void catalogs presented in [Douglass et al. \(2023\)](#). The catalogs were produced using a volume-limited sample of SDSS DR7 ($M_r \leq -20$, $z \leq 0.114$) with two popular void-finding algorithms implemented in the Void Analysis Software Toolkit (VAST; [Douglass et al. 2022](#)): `VoidFinder` and `V2`. `VoidFinder` ([El-Ad & Piran 1997](#)) is based on the growth and merging of nearly empty spheres, motivated by the expectation that voids are spherical to first order. `V2` (`Voronoi Voids`) is a Python 3 implementation of the `ZONES Bordering On Voidness`; [Neyrinck 2008](#)) algorithm, which defines voids based on local minima in the galactic density field. An example of the results from the VAST void-finding algorithms applied to SDSS DR7 are shown in [Figure 1](#). Any galaxy which falls within one of the void regions defined by a given algorithm is considered a void galaxy; all others are classified as wall galaxies.

4.1. `VoidFinder`

`VoidFinder` begins by identifying and removing all field galaxies, defined as those galaxies with their third nearest neighbor farther than $5.33h^{-1} \text{ Mpc}$. The remaining (wall) galaxies are placed on a three dimensional grid with side lengths of $5h^{-1} \text{ Mpc}$. Spheres are

¹ <http://www.nsatlas.org/>

² <https://wwwmpa.mpa-garching.mpg.de/SDSS/DR7/>

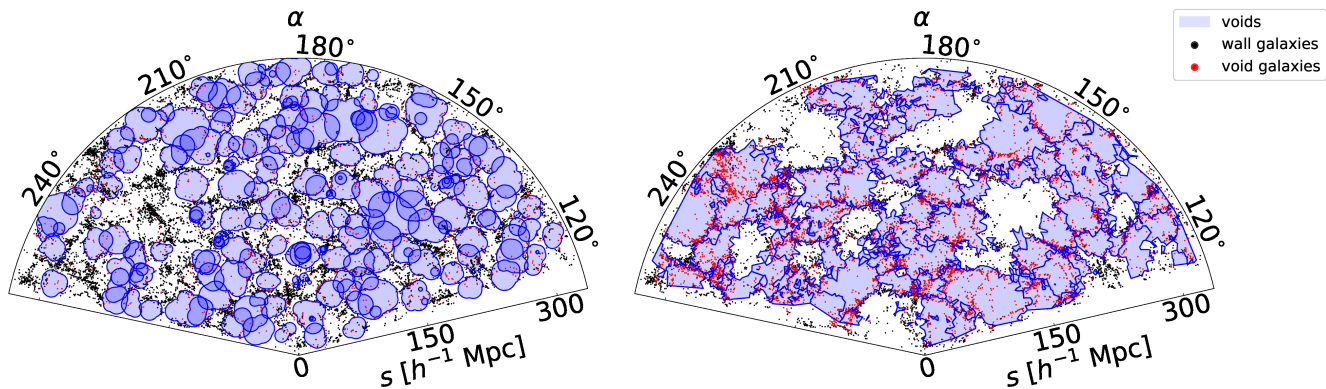


Figure 1. Results from VAST’s VoidFinder (left) and V^2 (right) for a $10h^{-1}$ Mpc-thick slice centered on declination $\delta = 32^\circ$ of the main SDSS DR7 galaxy catalog. The intersection of the midplane of the declination range and the voids are shown in blue; galaxies that fall within a void are colored in red, while those that do not are shown in black. Projection effects can produce void galaxies appearing to fall outside a void, and some wall galaxies appearing to fall within a void.

grown from the center of each empty grid cell and expand until they are bounded by four galaxies on their surface. Each void is defined as a union of these spheres, where the largest sphere within a void is that void’s maximal sphere. Maximal spheres are not permitted to overlap each other by more than 10% of their volume, and they have a minimum radius of $10h^{-1}$ Mpc. All other spheres of a given void must overlap only their void’s maximal sphere by at least 50% of their volumes. For more details, see Section A.1 and Douglass et al. (2023).

4.2. Voronoi Voids (V^2)

V^2 first produces a 3D Voronoi tessellation of the input galaxy catalog. The Voronoi cells are combined into “zones” using a watershed segmentation. Zones are then merged into voids if the least-dense pair of adjacent cells between two zones is below a given maximum “linking density.” Here, we define the zone-linking density threshold as $0.2\bar{\rho}$, where $\bar{\rho}$ is the mean density of the SDSS DR7 volume-limited galaxy catalog, similar to the threshold used in VIDE (Sutter et al. 2015). In addition, we prune our V^2 catalog to remove all voids with an effective radius smaller than $10h^{-1}$ Mpc. For more details, see Section A.2 and Douglass et al. (2023).

Unlike VoidFinder, which assumes that the voids are spherical to first order, V^2 makes no assumptions regarding void shape. In addition, V^2 depends on fewer tunable parameters than VoidFinder, making it more survey-agnostic.

5. COMPARISON OF VOID GALAXY PROPERTIES BETWEEN ALGORITHMS

We investigate the influence of the void environment on inferred galaxy properties, where the environmental classification (void or wall) is determined from each of the void catalogs described in Section 4. To study how the inferred properties of void galaxies depend on the choice of void-finding algorithm, we plot the distribution of each property for the void and wall galaxy populations as defined by VoidFinder and V^2 . We report the mean, median, and corresponding difference between the means and medians of the void and wall galaxy distributions for each property and algorithm in Table 1.

Two Bayesian analysis models are used to quantify the statistical significance of differences between the inferred properties of void and wall galaxies. Properties with unimodal distributions (luminosity and stellar mass) are modeled as a mixture of two skew normal distributions; properties with bimodal distributions (color and (s)SFR) are modeled as a mixture of three skew normal distributions. We then compute the Poisson likelihoods that the void and wall galaxy properties are drawn from the same parent distribution and from different parent populations. The likelihood ratio of the one- and two-parent models is used to construct a Bayes factor, B_{12} , to discriminate between the models (see Appendix A.3 for details).

For all properties and void-finding algorithms, the Bayes factor gives decisive evidence in favor of the two-parent model. However, the differences between void and wall galaxies are substantially less significant for V^2 than VoidFinder. The Bayes factors for all galaxy properties and void-finding algorithms are listed in the rightmost column of Table 1. In the following subsections, we describe differences between the stellar mass, color, luminosity, and (specific) star formation rate of void and wall galaxies using V^2 and VoidFinder for void galaxy classification.

Table 1. Galaxy property distribution statistics

| Algorithm | Environment | Average | Median | Average shift | Median shift | $\log_{10}(B_{12})$ |
|--------------------------------------|-------------|---------------------|---------|---|----------------|---------------------|
| Stellar mass [$\log(M_*/M_\odot)$] | | | | | | |
| VoidFinder | Void | 9.786 ± 0.002 | 9.910 | 0.205 ± 0.002 ($2.1 \pm 0.2\%$) | 0.164 (1.6%) | −1708 |
| | Wall | 9.992 ± 0.001 | 10.074 | | | |
| V ² | Void | 9.927 ± 0.001 | 10.025 | 0.038 ± 0.002 ($0.4 \pm 0.2\%$) | 0.043 (0.4%) | −203 |
| | Wall | 9.965 ± 0.002 | 10.068 | | | |
| Absolute magnitude, M_r | | | | | | |
| VoidFinder | Void | -19.619 ± 0.004 | −19.837 | -0.359 ± 0.005 ($1.8 \pm 0.5\%$) | −0.263 (1.3%) | −1248 |
| | Wall | -19.978 ± 0.002 | −20.100 | | | |
| V ² | Void | -19.859 ± 0.002 | −20.013 | -0.075 ± 0.005 ($0.4 \pm 0.5\%$) | −0.088 (0.4%) | −308 |
| | Wall | -19.934 ± 0.004 | −20.101 | | | |
| $u - r$ | | | | | | |
| VoidFinder | Void | 1.763 ± 0.002 | 1.730 | 0.173 ± 0.002 ($9.0 \pm 0.2\%$) | 0.259 (13%) | −1592 |
| | Wall | 1.937 ± 0.001 | 1.989 | | | |
| V ² | Void | 2.102 ± 0.001 | 2.127 | 0.027 ± 0.002 ($1.3 \pm 0.2\%$) | 0.039 (1.8%) | −28.8 |
| | Wall | 2.130 ± 0.002 | 2.166 | | | |
| $g - r$ | | | | | | |
| VoidFinder | Void | 0.5614 ± 0.0007 | 0.5729 | 0.0540 ± 0.0008 ($8.77 \pm 0.08\%$) | 0.0855 (13.0%) | −1704 |
| | Wall | 0.6154 ± 0.0004 | 0.6584 | | | |
| V ² | Void | 0.6836 ± 0.0005 | 0.7201 | 0.0128 ± 0.0009 ($1.84 \pm 0.09\%$) | 0.0172 (2.33%) | −57.9 |
| | Wall | 0.6963 ± 0.0007 | 0.7373 | | | |
| SFR [$\log(M_\odot/\text{yr})$] | | | | | | |
| VoidFinder | Void | -0.303 ± 0.002 | −0.216 | -0.097 ± 0.003 ($24.2 \pm 0.3\%$) | −0.175 (44.8%) | −416 |
| | Wall | -0.400 ± 0.001 | −0.391 | | | |
| V ² | Void | -0.385 ± 0.001 | −0.355 | 0.008 ± 0.003 ($2.1 \pm 0.3\%$) | 0.020 (5.9%) | −66.5 |
| | Wall | -0.377 ± 0.002 | −0.336 | | | |
| sSFR [$\log(\text{yr}^{-1})$] | | | | | | |
| VoidFinder | Void | -10.489 ± 0.003 | −10.232 | -0.294 ± 0.003 ($2.7 \pm 0.3\%$) | −0.445 (4.2%) | −1471 |
| | Wall | -10.783 ± 0.002 | −10.677 | | | |
| V ² | Void | -10.705 ± 0.002 | −10.521 | -0.044 ± 0.003 ($0.4 \pm 0.3\%$) | −0.094 (0.9%) | −18.9 |
| | Wall | -10.750 ± 0.003 | −10.615 | | | |

NOTE—Galaxy property distribution summary for void and wall environments according to **VoidFinder** or **V²**. The shifts are calculated as (wall − void), and the percentages are equal to (wall − void)/wall, with a negative sign indicating that void galaxies have larger values than the wall galaxies. The logarithm of the Bayes factor is included; all Bayes factors are significantly less than $\log(1/100) = -2$, indicating definitive evidence for the two-parent model (Appendix A.3).

5.1. *Stellar Mass*

We study the distribution of stellar masses of void galaxies compared to the distribution of galaxies in denser regions, as shown in Figure 2. Void galaxies are expected to have systematically lower stellar masses than galaxies in denser regions because galaxy interactions, much more rare in voids, are expected to enhance star formation. Both the distributions shown in Figure 2 and the statistics reported in Table 1 show that the stellar mass distribution for void galaxies is statistically different than the wall galaxy sample when either void-finding algorithm is used for void classification. When the void environment is defined with `VoidFinder`, we see this difference manifest as a relatively large shift towards lower stellar masses in the voids. With V^2 , though, we find that the difference between the void and wall populations is very slight and appears to be a result of a slight narrowing of the stellar mass distribution in walls, as the void galaxy distribution appears to match the distribution of all galaxies.

5.2. *Luminosity*

A galaxy’s luminosity is closely linked to its stellar mass, so we expect void galaxies to be systematically fainter than galaxies in denser regions. As seen on the left in Figure 3, the classification by `VoidFinder` results in a shift towards fainter luminosities for void galaxies than galaxies in denser environments. This matches the trend observed in the stellar mass, shown in Figure 2. Using the V^2 void catalog, though, we see very little difference between the void and wall galaxy luminosity distributions, as seen on the right in Figure 3; the void galaxies as defined by V^2 have nearly the same luminosities as its wall galaxies, with possibly a slight thinning of the wall population. The Bayes factors (listed in Table 1) corroborate these differences between the void and wall populations for both classifications.

5.3. *(specific) Star formation rate*

Void galaxies are expected to be undergoing more star formation today than galaxies in denser regions, due both to potential retarded star formation and their continued presence of cold gas reservoirs (Cen 2011). Therefore, void galaxies are expected to have higher star formation rates (SFR) and specific star formation rates (sSFR; the star formation rate per unit mass) than galaxies in denser regions. As shown in the left column of Figure 4, we find that void galaxies have higher (s)SFR values relative to galaxies in denser environments when using the `VoidFinder` void catalog for environmental classification. As seen on the right in Figure 4, the distributions for V^2 show no such trend in

(s)SFR — according to the V^2 void catalog, both void and wall galaxies have the same (s)SFR.

The Bayes factors (listed in Table 1) support the significant difference between the void and wall populations of `VoidFinder` for the (s)SFR distributions. However, the Bayes factors for the (s)SFR distributions for void and wall galaxies as classified by V^2 also indicate that the two populations come from different parent distributions. From the distributions shown on the right in Figure 4, this is possibly due to a very slight shift in the V^2 wall galaxy population towards lower (s)SFRs, not a shift in the void galaxy population towards higher (s)SFRs as seen with `VoidFinder`.

5.4. *Color*

For galaxies in SDSS DR7, we explore the distribution of the color of void galaxies relative to galaxies in denser regions as classified by both `VoidFinder` and V^2 , as shown in Figure 5. A galaxy’s color is determined by its stellar populations: bluer colors are a result of hot O and B stars, indicating that star formation has recently occurred, and red colors are indicative of an old stellar population. With star formation expected to shift to later times in void regions, void galaxies are expected to be systematically bluer than galaxies in denser regions. This is exactly the shift that we see in the `VoidFinder` void galaxy population, shown on the left in Figure 5 and reflected in the Bayes factor reported in Table 1 comparing the `VoidFinder` galaxy distributions.

The Bayes factors for the V^2 color distributions are two orders of magnitude smaller than those of `VoidFinder`. Combined with the distributions shown on the right in Figure 5, we conclude that the differences quantified by the Bayes factors in the V^2 distributions are actually a result of a slight increase in redder galaxies in the wall population, as evidenced by the slight increase in amplitude of the right-hand peak and slight decrease in the left-hand peak of the V^2 wall distributions compared to the void and overall distributions.

6. DISCUSSION

In Section 5, we compare the distributions of a range of galaxy properties for galaxies in voids and galaxies in denser regions using two different definitions of the void environment. With `VoidFinder`, we find that void galaxies are systematically fainter, bluer, less massive, and have considerably higher star formation rates than galaxies in denser regions. With V^2 , though, we see very little difference between the properties of void galaxies and the properties of galaxies in denser regions.

6.1. *Impact of the void-finding algorithm on galaxy classification*

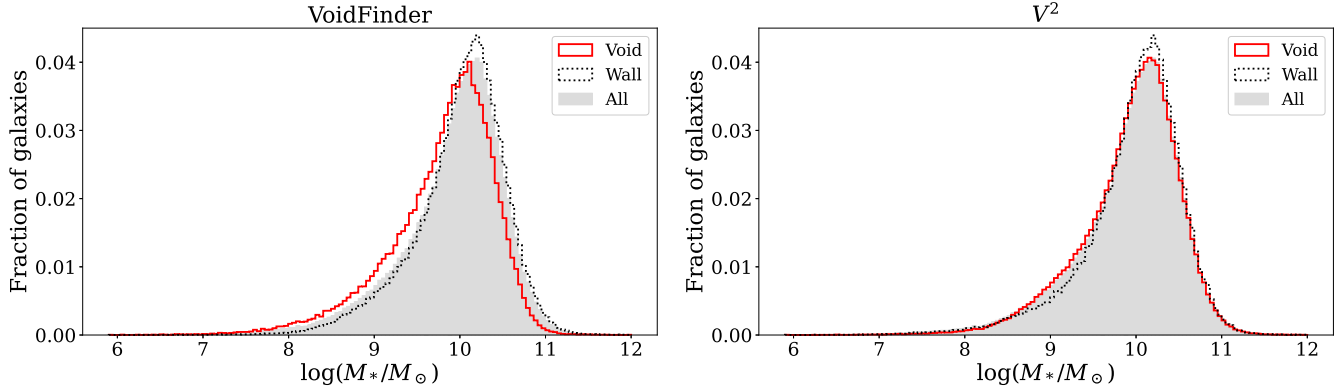


Figure 2. Stellar mass distribution of galaxies, separated into void and wall environments according to the `VoidFinder` (left) and V^2 (right) void catalogs. The distribution of all galaxies is shaded in gray. There is a shift towards lower stellar mass for void galaxies relative to wall galaxies with both void classifications, although V^2 's is very slight.

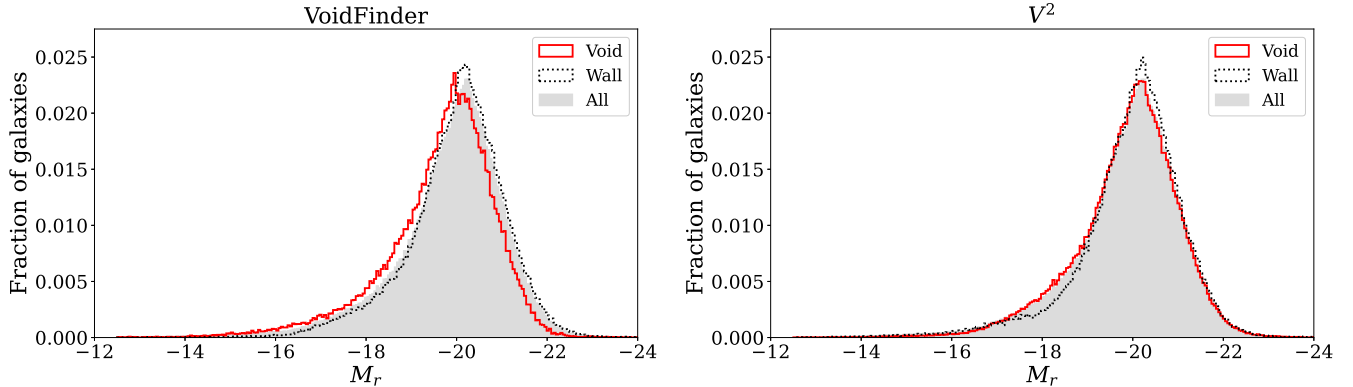


Figure 3. Luminosity distribution of galaxies separated according to void and wall environments by `VoidFinder` (left) and V^2 (right). The distribution for all galaxies is shaded in gray. There is a shift towards fainter luminosities in the distribution of void galaxies relative to wall galaxies in `VoidFinder`'s classification, while it appears that the wall galaxies are shifted towards slightly brighter luminosities with V^2 's classification.

The Λ CDM cosmology predicts void galaxies to be retarded in their star formation relative to galaxies in denser regions since they experience fewer interactions (which often initiate star formation episodes) compared to galaxies in denser regions. Additionally, they are able to retain their gas as they evolve in these extremely underdense environments (Cen 2011), allowing them to continue forming stars up to the present epoch. The void galaxy properties with `VoidFinder` used to define void regions are therefore consistent with the simulated physical properties of void galaxies (Benson et al. 2003; Cen 2011; Habouzit et al. 2020; Peper & Roukema 2021) and with previous observations: void galaxies are fainter (e.g., Croton et al. 2005; Hoyle et al. 2005; Sorrentino et al. 2006; Kreckel et al. 2012; Moorman et al. 2015), less massive (e.g., Jung et al. 2014; Alpaslan et al. 2016; Beygu et al. 2017; Martizzi et al. 2020), bluer (e.g., Groggin & Geller 1999; Rojas et al. 2004; Croton et al. 2005; Patiri et al. 2006; Sorrentino et al. 2006; von Benda-

Beckmann & Müller 2008; Hoyle et al. 2012; Kreckel et al. 2012), and have higher (s)SFR (e.g., Rojas et al. 2005; von Benda-Beckmann & Müller 2008; Cybulski et al. 2014; Liu et al. 2015; Beygu et al. 2016; Moorman et al. 2016).

However, we do not see these expected traits for galaxies in voids defined by V^2 . To better understand the source of this discrepancy, we investigate the V^2 void galaxies in more detail. We find that 23.4% of `VoidFinder` wall galaxies are classified as void galaxies by V^2 , and 40.5% of V^2 void galaxies are classified as wall galaxies by `VoidFinder`. As described in Section 4, `VoidFinder` voids are found by expanding spheres until they reach a relatively bright galaxy that is not isolated, while V^2 defines voids by connecting Voronoi cells until they reach local density maxima. Since these density maxima are likely to be close to the centers of the walls/filaments rather than their edges (where the brighter non-isolated galaxies that `VoidFinder` stops

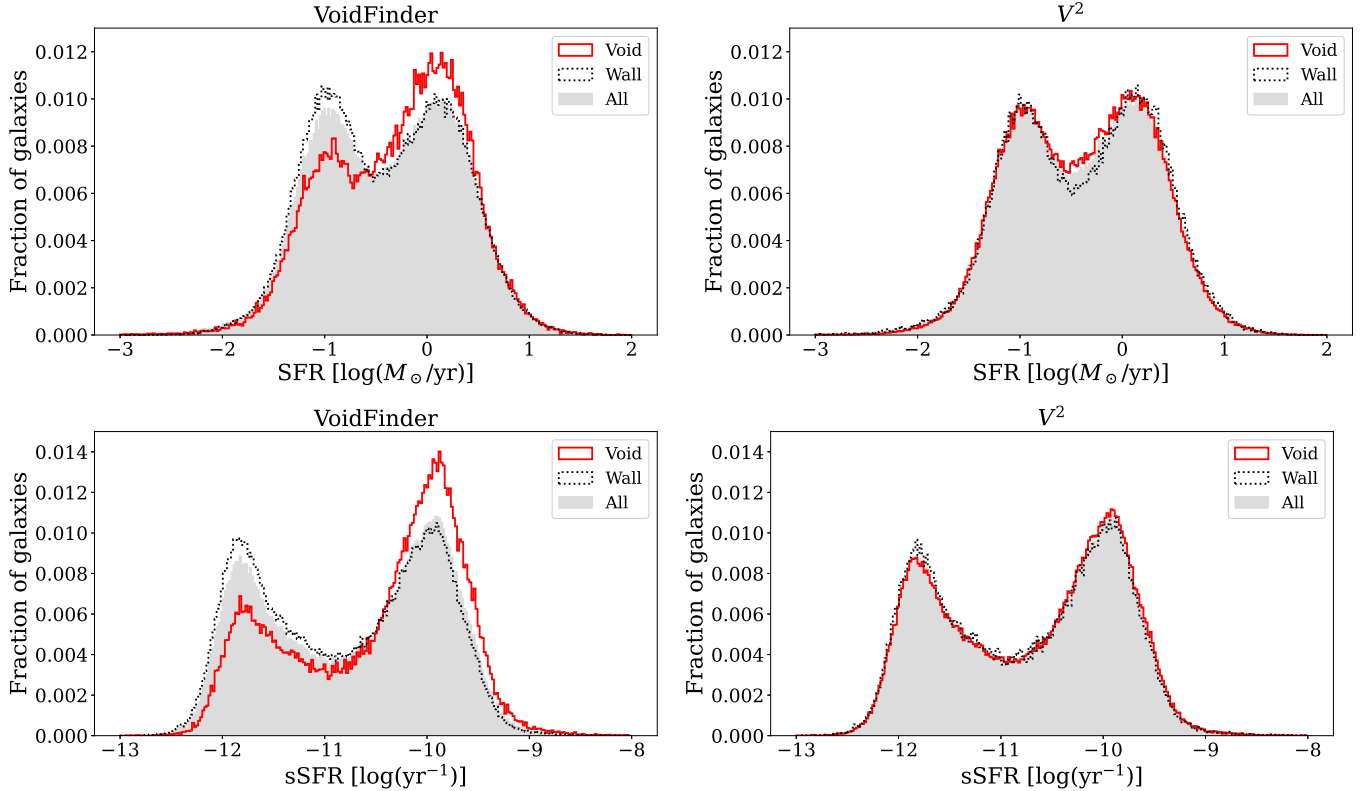


Figure 4. Star formation rate (SFR, top) and specific star formation rate (sSFR, bottom) distributions of galaxies for void and wall environments as classified by VoidFinder (left) and V^2 (right). The distribution of all galaxies is shown in gray for comparison. When classified using VoidFinder’s void catalog, void galaxies have systematically higher (specific) star formation rates relative to wall galaxies; we observe no discernible difference between void and wall galaxies when the V^2 void catalog is used.

at are located), V^2 likely extends further into what VoidFinder considers a wall. This leads to V^2 classifying many galaxies as void that are, instead, classified as wall galaxies by VoidFinder.

Considering how the algorithms define the edges of voids and how VoidFinder’s results are consistent with expectations, we conclude that the void environment of V^2 is contaminated by wall galaxies, similar to that shown by Florez et al. (2021) and Veyrat et al. (2023). V^2 ’s void environment is therefore expected to behave more like the general distribution of galaxies. Our observations agree with the simulation results of Veyrat et al. (2023): VoidFinder provides a better delineation between the dynamically-distinct void regions and the surrounding wall structures, leading to more reasonable physical conclusions regarding the properties of void galaxies. Unless additional restrictions are implemented, this contamination results in the void-wall classification from V^2 , and thus ZOBOV-like algorithms, to not be suitable for void environment studies of galaxy formation and evolution.

6.2. Galaxy properties as a function of depth within V^2 voids

If the void samples of V^2 are contaminated by wall galaxies located at the edges of its voids, the expected void galaxy properties can be recovered by focusing on the galaxies that are closer to the centers of its voids. Studying the galaxy properties as a function of void depth, we can determine the void depth within which V^2 void galaxies have similar trends to VoidFinder void galaxies. This is the observational complement to one of the mitigation techniques discussed in Veyrat et al. (2023), who tested this idea on the dynamical classification of simulated dark matter particles.

We calculate a galaxy’s distance to the void’s edge to determine how deep a galaxy is within a V^2 void. This is equivalent to the distance from the position of the galaxy to the edge of the void, defined by the Voronoi-cell surfaces that make up the boundary between a cell inside the void and a cell outside of it. We normalize the depth of each galaxy by the largest depth calculated for that void, so that we can compare voids of different sizes. Therefore, the deepest galaxy within each void

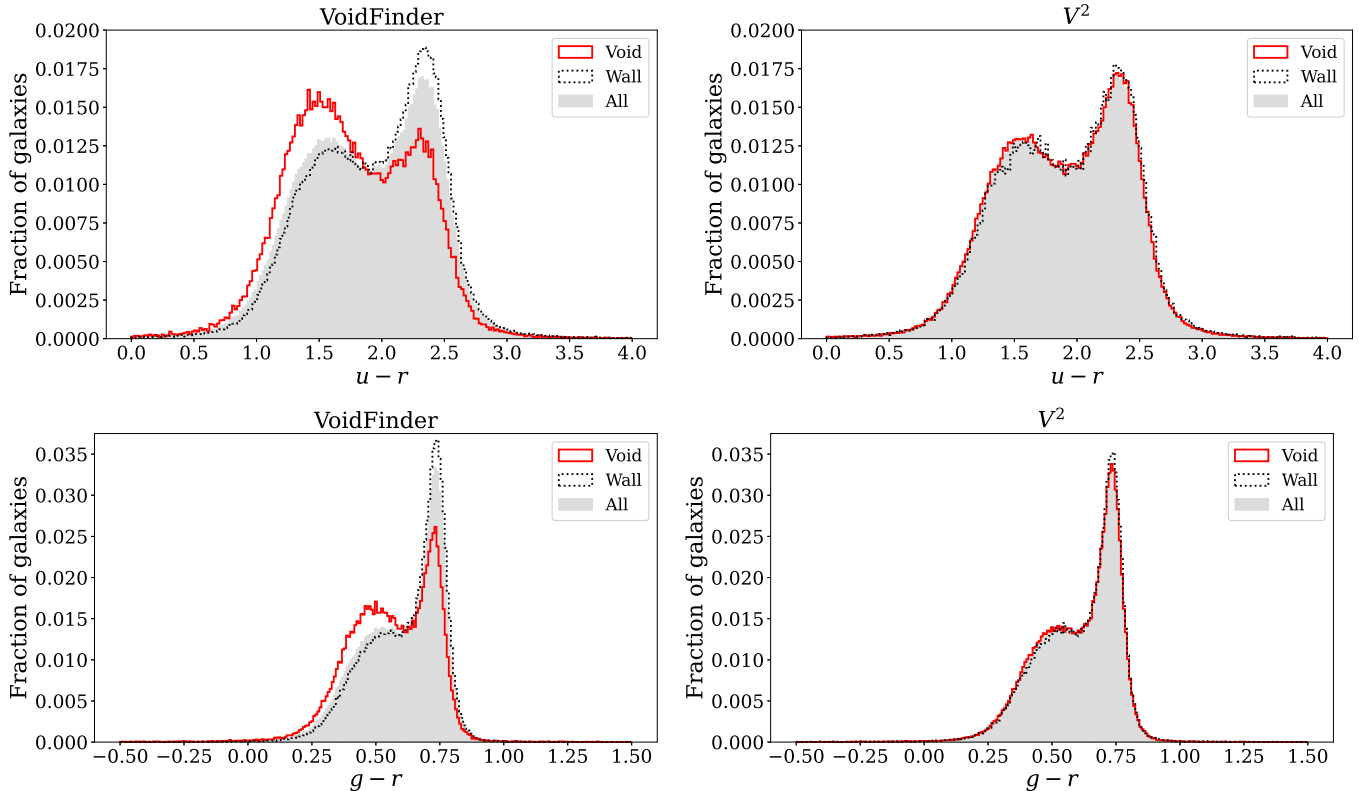


Figure 5. Color distribution, $u - r$ (top row) and $g - r$ (bottom row), separated by their environment (void, wall) using VoidFinder (left column) and V^2 (right column). The distribution for all galaxies is given in gray. There is an apparent shift towards bluer color for void galaxies relative to wall galaxies with VoidFinder’s classification but not V^2 ’s.

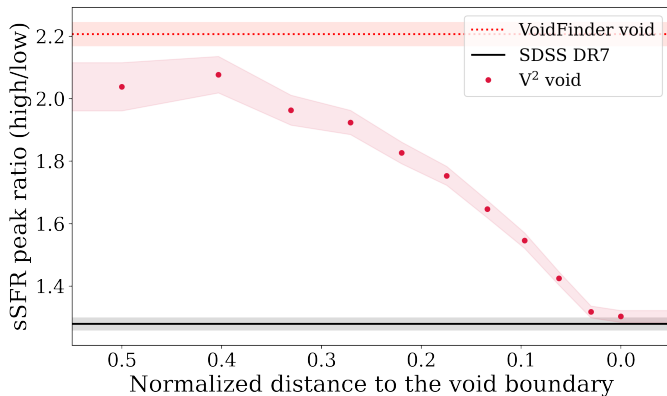


Figure 6. The relationship between the distribution of sSFR of void galaxies, as classified by V^2 , and the galaxies’ depths within the voids in which they reside (whether they live close to the edge of the void or deep inside it). The deepest galaxies within each void have a normalized distance of 1, while a distance closer to 0 indicates galaxies that are close to the edge. Galaxies further from the edges of the V^2 voids have sSFR distributions which more closely match that of VoidFinder void galaxies; as galaxies closer to the V^2 void boundaries are included in the sample, the sSFR distribution shifts to more closely resemble the SDSS DR7 galaxy distribution.

has a depth of 1, and a galaxy close to the edge will have a depth close to 0.

To test this hypothesis, we fit subsets of the V^2 void galaxies with a skew normal (or sum of two skew normals if the distribution is bimodal) as a function of void depth for each galaxy property studied in Section 5. For a given void depth, the corresponding subsample of void galaxies consists of all galaxies with depths greater than the given depth threshold. This allows us to study the behavior of the V^2 void galaxy population if the voids were limited to some inner fraction of the current total void size. The results of this analysis for the sSFR is shown in Figure 6. For comparison, we also include the ratio of the sSFR peak amplitudes for VoidFinder void galaxies (in red) and the ratio of the sSFR peak amplitudes for all galaxies in the overall NSA catalog (in black).

For unimodal galaxy properties (stellar mass and luminosity), we find a steady shift from smaller masses / fainter luminosities to larger masses / brighter luminosities as the V^2 void galaxies include more of those closer to the void boundaries. For properties with bimodal distributions (color and (s)SFR), the fraction of blue galaxies / galaxies with higher (s)SFR decreases

while the fraction of red galaxies / galaxies with lower (s)SFR increases as we include more V^2 void galaxies closer to their void boundaries. Figure 6 shows the ratio of the peak of the mode at higher sSFR to the mode at lower sSFR as a function of minimum depth included in the subsample.

For all properties, we find that the V^2 void galaxy distribution matches that of `VoidFinder` void galaxies when only V^2 void galaxies in the inner $\sim 20\%$ of the volume of the V^2 voids are included in the void sample. Therefore, the galaxies sitting close to the boundaries of V^2 voids are more likely to be wall galaxies and not actual void galaxies. This matches the results of [Habouzit et al. \(2020\)](#), who apply `VIDE` to a cosmological hydrodynamical simulation and reproduce the expected void galaxy property results when including only those galaxies closest to the centers of the `VIDE` voids. This also matches the simulation results of [Veyrat et al. \(2023\)](#), who compare the distribution of dark matter particles with a given crossing number as a function of void depth for both `VoidFinder` and V^2 . [Nadathur & Hotchkiss \(2014\)](#) also discusses the tendency for the watershed algorithm to include high-density walls and filaments within void regions.

Therefore, our analysis of galaxy properties as a function of depth within V^2 voids is consistent with our hypothesis and previous studies that the void sample of V^2 is contaminated by wall galaxies, a result of the extension of V^2 voids into the walls. This is visible on the right in Figure 1, where clustered void galaxies (in red) are located at the void edges. This phenomenon is also visible in our mock 2D galaxy catalog (see the middle and right panels of Figure 9), where multiple cells outside the artificial voids are joined to the void region. This “leaking” of the void regions into the walls is a consequence of how the watershed algorithm within V^2 (and other `ZOBOV`-like void-finders) defines void boundaries based on density maxima. To use V^2 voids to study galaxy properties, one must therefore implement a depth limit to exclude wall galaxies from the void galaxy population.

7. CONCLUSIONS

We examine the impact of the choice of void-finding algorithm used to classify the large-scale structure of galaxies by comparing properties of galaxies determined to be void galaxies using the `VoidFinder` and V^2 algorithms. Using the `VoidFinder` void catalog for SDSS DR7, we find that the distributions of void galaxy properties are consistent with the expected physical

properties of galaxies existing in voids: smaller masses, fainter luminosities, bluer colors, and higher (specific) star formation rates. When using V^2 , however, we find very little difference between the properties of void galaxies and the properties of galaxies in denser regions.

Upon further investigation, we find that V^2 void regions include a significant fraction of the walls and filaments. This is a result of the watershed algorithm extending void regions to the galaxy density maxima, which are located in the centers of the denser regions in the galaxy distribution. While `VoidFinder` is better suited for studying void galaxy properties because it is not subject to this phenomenon, it is possible to recover the void galaxy population with V^2 voids if voids are limited to the inner $\sim 20\%$ of their volume.

8. ACKNOWLEDGEMENTS

The authors thank Stephen W. O’Neill, Jr. for his help and expertise with `VAST`, as well as Michael Vogele, Regina Demina, and Tom Ferbel for their feedback on this manuscript. D. Veyrat and S. BenZvi acknowledge support from the U.S. Department of Energy Office of High Energy Physics under the Award Number DE-SC0008475.

Funding for the SDSS and SDSS-II has been provided by the Alfred P. Sloan Foundation, the Participating Institutions, the National Science Foundation, the U.S. Department of Energy, the National Aeronautics and Space Administration, the Japanese Monbukagakusho, the Max Planck Society, and the Higher Education Funding Council for England. The SDSS web site is <http://www.sdss.org/>.

The SDSS is managed by the Astrophysical Consortium for the Participating Institutions. The Participating Institutions are the American Museum of Natural History, Astrophysical Institute Potsdam, University of Basel, University of Cambridge, Case Western Reserve University, University of Chicago, Drexel University, Fermilab, the Institute for Advanced Study, the Japan Participation Group, Johns Hopkins University, the Joint Institute for Nuclear Astrophysics, the Kavli Institute for Particle Astrophysics and Cosmology, the Korean Scientist Group, the Chinese Academy of Sciences (LAMOST), Los Alamos National Laboratory, the Max-Planck-Institute for Astronomy (MPIA), the Max-Planck-Institute for Astrophysics (MPA), New Mexico State University, Ohio State University, University of Pittsburgh, University of Portsmouth, Princeton University, the United States Naval Observatory, and the University of Washington.

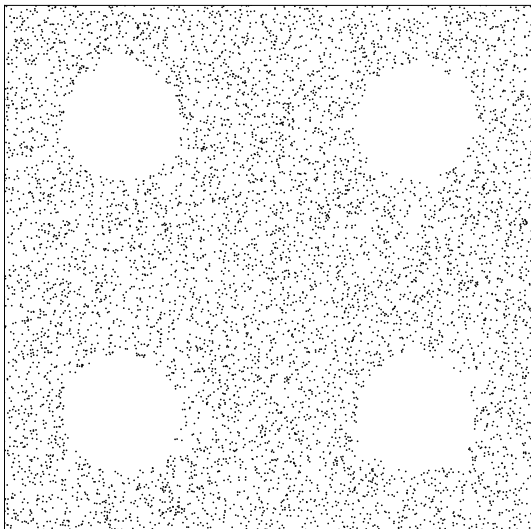


Figure 7. A sample random 2D galaxy catalog with circles of radius $10\bar{r}$ removed in each quadrant to simulate simple voids, where \bar{r} is the mean inter-particle separation.

A. VAST EXAMPLES

To visualize how the two algorithms included in VAST identify voids, we apply each algorithm to a two-dimensional (2D) mock catalog of randomly distributed galaxies. The artificial voids are formed by emptying four circular holes in the random galaxy distribution, as shown in Figure 7.

A.1. *VoidFinder* example

After removing isolated (field) galaxies, the remaining (wall) galaxies are placed on a $5h^{-1}$ Mpc grid. An example of this grid is shown on the left in Figure 8 for the 2D mock galaxies, where empty cells are colored blue.

Next, a sphere (or hole) is expanded from each empty cell in the grid. Each sphere, centered on the cell, is created with radius equal to the distance to the nearest wall galaxy. The sphere’s center then shifts away from that galaxy as its radius increases until its surface encounters a second galaxy. At this point, the sphere expands from the midpoint between these two galaxies until a third galaxy is encountered. Finally, the sphere grows perpendicularly away from the plane formed by these three galaxies until it reaches a fourth galaxy. The center panel of Figure 8 shows the result of this step for the 2D catalog of mock galaxies.

To extract unique voids from this list of holes, the holes are sorted by radius, and the largest hole is iden-

tified as a maximal sphere — the largest sphere that can fit in a given void region. Then, for each subsequent hole, if it does not overlap any already-identified maximal spheres by more than 10% of its volume, it is also identified as a maximal sphere. This process continues for all holes with radii larger than $10\bar{r}$, where \bar{r} is the mean particle separation in the simulated random sample.

Finally, the volume of the void is refined by merging each maximal sphere with the remaining non-maximal spheres. When a hole overlaps only one maximal sphere by more than 50% of its volume, it is merged into that void. Holes that overlap multiple maximal spheres by more than 50% are discarded. Each void is therefore composed of one maximal sphere and some number of smaller holes. The right panel in Figure 8 shows the final 2D catalog of voids found using *VoidFinder*.

A.2. v^2 example

v^2 can be divided into four steps:

1. **Tessellation:** A Voronoi tessellation of the input catalog is produced. The tessellation of the 2D mock galaxies is shown on the left in Figure 9. The inverse of each cell’s volume is an estimate of that galaxy’s local density.
2. **Zone formation:** Voronoi cells are combined into groups or “zones” using watershed segmentation. Each cell is put into the same zone as its least-dense neighbor, and cells less dense than any neighboring cell (local density minima) are identified as their zone’s central cell. The center panel of Figure 9 shows the zones formed using the 2D mock sample.
3. **Zone merging:** Zones are merged to form voids by first identifying the least-dense pair of adjacent cells between two zones. For a given maximum “linking density,” the set of all zones is partitioned into a subset of voids linked together by zones of equal or lower density. The algorithm then loops over all linking densities to produce a list of voids.
4. **Void pruning:** Zone linking produces a hierarchy of voids ranging from individual zones to a single void encompassing the entire survey volume. A pruning step similar to that implemented in VIDE (Sutter et al. 2015) is therefore introduced to identify the final list of voids. The final result for the 2D sample with this pruning is shown on the right in Figure 9.

A.3. *Calculating the Bayes factor*

Due to our large sample size, non-Bayesian significance tests such as a two-sample Kolmogorov–Smirnov

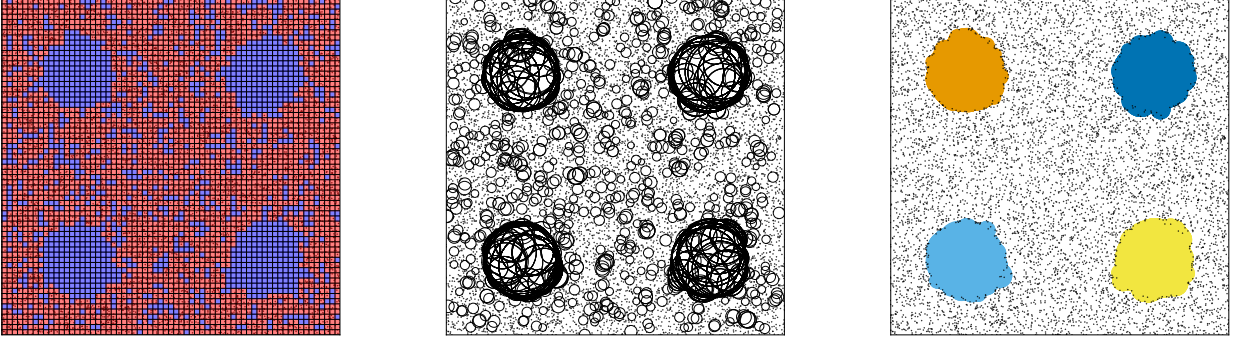


Figure 8. Steps in the VoidFinder algorithm applied to a 2D mock galaxy catalog. *Left:* Non-field (wall) galaxies placed on a grid. Any grid cell containing at least one galaxy is shaded red; all empty grid cells are blue. *Center:* Circles grown from the center of each empty grid cell until bounded by at least three galaxies. *Right:* Voids formed through the union of the grown spheres.

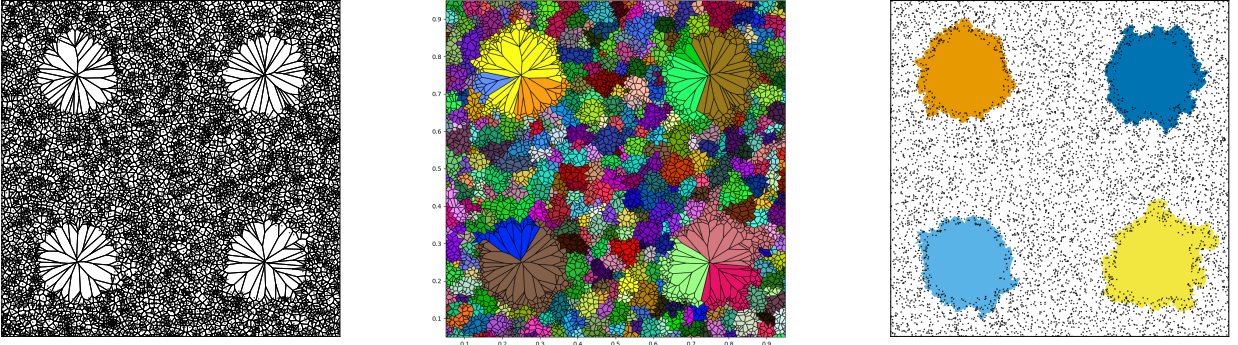


Figure 9. Steps in the V^2 algorithm applied to a 2D mock galaxy catalog. *Left:* The Voronoi tessellation of the catalog. *Center:* Zones formed using a watershed method. *Right:* Final voids identified after merging zones and pruning voids.

(K-S) test yield extremely low p-values that inaccurately quantify the extent of similarity of our distributions. Since we know that our data is distributed like one or more Gaussian or skew normal distributions (a mixture model), we can bin and fit the data to the model assuming that the samples come from either the same parent distribution or two different parent distributions. Then, we can compare these two models using the Bayes Factor.

We have two data sets with binned counts $\mathbf{m} = m_i$ and $\mathbf{n} = n_i$. For the single-parent model, we assume that both data sets are created by the same skew normal mixture model, such that the mean count in bin i for data set 1 is

$$\lambda_{1,i} = [\alpha \text{SN}(\mu_\alpha, \sigma_\alpha, \xi_\alpha) + \beta \text{SN}(\mu_\beta, \sigma_\beta, \xi_\beta)]_i. \quad (\text{A1})$$

To account for the different sizes in the data sets, we can add a scale factor s to the fit of the second data set:

$$\lambda_{2,i} = [s(\alpha \text{SN}(\mu_\alpha, \sigma_\alpha, \xi_\alpha) + \beta \text{SN}(\mu_\beta, \sigma_\beta, \xi_\beta))]_i = s\lambda_{1,i}. \quad (\text{A2})$$

Thus the model includes 9 parameters $\theta = \{s, \alpha, \mu_\alpha, \sigma_\alpha, \xi_\alpha, \beta, \mu_\beta, \sigma_\beta, \xi_\beta\}$. We can then maximize the joint Poisson likelihood

$$p(\mathbf{m}, \mathbf{n} | \lambda_1, \lambda_2, \mathcal{M}_1) = \prod_{i=1}^N \frac{\lambda_{1,i}^{m_i} e^{-\lambda_{1,i}}}{m_i!} \frac{\lambda_{2,i}^{n_i} e^{-\lambda_{2,i}}}{n_i!}, \quad (\text{A3})$$

or minimize the negative log likelihood

$$-\ln \mathcal{L} = - \sum_{i=1}^N (m_i \lambda_{1,i} - \lambda_{1,i} - \ln m_i! + n_i \lambda_{2,i} - \lambda_{2,i} - \ln n_i!) \quad (\text{A4})$$

to obtain the best-fit parameters.

If on the other hand we assume the binned counts $\mathbf{m} = m_i$ and $\mathbf{n} = n_i$ are created by separate skew normal mixture models with mean count

$$\lambda_{1,i} = [\alpha \text{SN}(\mu_\alpha, \sigma_\alpha, \xi_\alpha) + \beta \text{SN}(\mu_\beta, \sigma_\beta, \xi_\beta)]_i \quad (\text{A5})$$

in set 1 and mean count

$$\lambda_{2,i} = [\gamma \text{SN}(\mu_\gamma, \sigma_\gamma, \xi_\gamma) + \delta \text{SN}(\mu_\delta, \sigma_\delta, \xi_\delta)]_i \quad (\text{A6})$$

in set 2, then the model includes 16 free parameters

$$\theta = \{\alpha, \mu_\alpha, \sigma_\alpha, \xi_\alpha, \beta, \mu_\beta, \sigma_\beta, \xi_\beta, \gamma, \mu_\gamma, \sigma_\gamma, \xi_\gamma, \delta, \mu_\delta, \sigma_\delta, \xi_\delta\}.$$

We can still use the likelihood in Eqn. A3 with mean counts from Eqns. A5 and A6.

To evaluate the support of the Bayes factor for the one or two-parent hypothesis, we use the thresholds suggested in Jeffreys (1961) and Kass & Raftery (1995).

REFERENCES

- Abazajian, K. N., Adelman-McCarthy, J. K., Agüeros, M. A., et al. 2009, *ApJS*, 182, 543, doi: [10.1088/0067-0049/182/2/543](https://doi.org/10.1088/0067-0049/182/2/543)
- Alpaslan, M., Grootes, M., Marcum, P. M., et al. 2016, *MNRAS*, 457, 2287, doi: [10.1093/mnras/stw134](https://doi.org/10.1093/mnras/stw134)
- Benson, A. J., Hoyle, F., Torres, F., & Vogeley, M. S. 2003, *MNRAS*, 340, 160, doi: [10.1046/j.1365-8711.2003.06281.x](https://doi.org/10.1046/j.1365-8711.2003.06281.x)
- Beygu, B., Kreckel, K., van der Hulst, J. M., et al. 2016, *MNRAS*, 458, 394, doi: [10.1093/mnras/stw280](https://doi.org/10.1093/mnras/stw280)
- Beygu, B., Peletier, R. F., van der Hulst, J. M., et al. 2017, *MNRAS*, 464, 666, doi: [10.1093/mnras/stw2362](https://doi.org/10.1093/mnras/stw2362)
- Blanton, M. R., Kazin, E., Muna, D., Weaver, B. A., & Price-Whelan, A. 2011, *AJ*, 142, 31, doi: [10.1088/0004-6256/142/1/31](https://doi.org/10.1088/0004-6256/142/1/31)
- Blanton, M. R., Lin, H., Lupton, R. H., et al. 2003, *AJ*, 125, 2276, doi: [10.1086/344761](https://doi.org/10.1086/344761)
- Bond, J. R., Kofman, L., & Pogosyan, D. 1996, *Nature*, 380, 603, doi: [10.1038/380603a0](https://doi.org/10.1038/380603a0)
- Brinchmann, J., Charlot, S., White, S. D. M., et al. 2004, *MNRAS*, 351, 1151, doi: [10.1111/j.1365-2966.2004.07881.x](https://doi.org/10.1111/j.1365-2966.2004.07881.x)
- Cen, R. 2011, *ApJ*, 741, 99, doi: [10.1088/0004-637X/741/2/99](https://doi.org/10.1088/0004-637X/741/2/99)
- Colberg, J. M., Pearce, F., Foster, C., et al. 2008, *MNRAS*, 387, 933, doi: [10.1111/j.1365-2966.2008.13307.x](https://doi.org/10.1111/j.1365-2966.2008.13307.x)
- Constantin, A., Hoyle, F., & Vogeley, M. S. 2008, *ApJ*, 673, 715, doi: [10.1086/524310](https://doi.org/10.1086/524310)
- Croton, D. J., Farrar, G. R., Norberg, P., et al. 2005, *MNRAS*, 356, 1155, doi: [10.1111/j.1365-2966.2004.08546.x](https://doi.org/10.1111/j.1365-2966.2004.08546.x)
- Cybulski, R., Yun, M. S., Fazio, G. G., & Gutermuth, R. A. 2014, *MNRAS*, 439, 3564, doi: [10.1093/mnras/stu200](https://doi.org/10.1093/mnras/stu200)
- de Lapparent, V., Geller, M. J., & Huchra, J. P. 1986, *ApJL*, 302, L1, doi: [10.1086/184625](https://doi.org/10.1086/184625)
- Douglass, K., Veyrat, D., O'Neill, S., et al. 2022, *JOSS*, 7, 4033, doi: [10.21105/joss.04033](https://doi.org/10.21105/joss.04033)
- Douglass, K. A., Veyrat, D., & BenZvi, S. 2023, *ApJS*, 265, 7, doi: [10.3847/1538-4365/acabcf](https://doi.org/10.3847/1538-4365/acabcf)
- Douglass, K. A., & Vogeley, M. S. 2017, *ApJ*, 837, 42, doi: [10.3847/1538-4357/aa5e53](https://doi.org/10.3847/1538-4357/aa5e53)
- El-Ad, H., & Piran, T. 1997, *ApJ*, 491, 421, doi: [10.1086/304973](https://doi.org/10.1086/304973)
- Florez, J., Berlind, A. A., Kannappan, S. J., et al. 2021, *ApJ*, 906, 97, doi: [10.3847/1538-4357/abca9f](https://doi.org/10.3847/1538-4357/abca9f)
- Grogin, N. A., & Geller, M. J. 1999, *AJ*, 118, 2561, doi: [10.1086/301126](https://doi.org/10.1086/301126)
- . 2000, *AJ*, 119, 32, doi: [10.1086/301179](https://doi.org/10.1086/301179)
- Habouzit, M., Pisani, A., Goulding, A., et al. 2020, *MNRAS*, 493, 899, doi: [10.1093/mnras/staa219](https://doi.org/10.1093/mnras/staa219)
- Hamaus, N., Pisani, A., Choi, J.-A., et al. 2020, *JCAP*, 2020, 023, doi: [10.1088/1475-7516/2020/12/023](https://doi.org/10.1088/1475-7516/2020/12/023)
- Hamaus, N., Pisani, A., Sutter, P. M., et al. 2016, *PhRvL*, 117, 091302, doi: [10.1103/PhysRevLett.117.091302](https://doi.org/10.1103/PhysRevLett.117.091302)
- Hoyle, F., Rojas, R. R., Vogeley, M. S., & Brinkmann, J. 2005, *ApJ*, 620, 618, doi: [10.1086/427176](https://doi.org/10.1086/427176)
- Hoyle, F., Vogeley, M. S., & Pan, D. 2012, *MNRAS*, 426, 3041, doi: [10.1111/j.1365-2966.2012.21943.x](https://doi.org/10.1111/j.1365-2966.2012.21943.x)
- Jeffreys, H. 1961, *Theory of Probability*, 3rd edn. (Oxford, UK: Oxford University Press)
- Jung, I., Lee, J., & Yi, S. K. 2014, *ApJ*, 794, 74, doi: [10.1088/0004-637X/794/1/74](https://doi.org/10.1088/0004-637X/794/1/74)
- Kass, R. E., & Raftery, A. E. 1995, *Journal of the American Statistical Association*, 90, 773, doi: [10.1080/01621459.1995.10476572](https://doi.org/10.1080/01621459.1995.10476572)
- Kreckel, K., Platen, E., Aragón-Calvo, M. A., et al. 2012, *AJ*, 144, 16, doi: [10.1088/0004-6256/144/1/16](https://doi.org/10.1088/0004-6256/144/1/16)
- Lavaux, G., & Wandelt, B. D. 2012, *ApJ*, 754, 109, doi: [10.1088/0004-637X/754/2/109](https://doi.org/10.1088/0004-637X/754/2/109)
- Liu, C.-X., Pan, D. C., Hao, L., et al. 2015, *ApJ*, 810, 165, doi: [10.1088/0004-637X/810/2/165](https://doi.org/10.1088/0004-637X/810/2/165)
- Lupton, R., Gunn, J. E., Ivezić, Z., Knapp, G. R., & Kent, S. 2001, in *Astronomical Society of the Pacific Conference Series*, Vol. 238, *Astronomical Data Analysis Software and Systems X*, ed. F. R. Harnden, Jr., F. A. Primini, & H. E. Payne, 269
- Mao, Q., Berlind, A. A., Scherrer, R. J., et al. 2017, *ApJ*, 835, 160, doi: [10.3847/1538-4357/835/2/160](https://doi.org/10.3847/1538-4357/835/2/160)

- Martizzi, D., Vogelsberger, M., Torrey, P., et al. 2020, MNRAS, 491, 5747, doi: [10.1093/mnras/stz3418](https://doi.org/10.1093/mnras/stz3418)
- Moorman, C. M., Moreno, J., White, A., et al. 2016, ApJ, 831, 118, doi: [10.3847/0004-637X/831/2/118](https://doi.org/10.3847/0004-637X/831/2/118)
- Moorman, C. M., Vogeley, M. S., Hoyle, F., et al. 2015, ApJ, 810, 108, doi: [10.1088/0004-637X/810/2/108](https://doi.org/10.1088/0004-637X/810/2/108)
- Muldrew, S. I., Croton, D. J., Skibba, R. A., et al. 2012, MNRAS, 419, 2670, doi: [10.1111/j.1365-2966.2011.19922.x](https://doi.org/10.1111/j.1365-2966.2011.19922.x)
- Nadathur, S., Carter, P. M., Percival, W. J., Winther, H. A., & Bautista, J. E. 2019, PhRvD, 100, 023504, doi: [10.1103/PhysRevD.100.023504](https://doi.org/10.1103/PhysRevD.100.023504)
- Nadathur, S., & Hotchkiss, S. 2014, MNRAS, 440, 1248, doi: [10.1093/mnras/stu349](https://doi.org/10.1093/mnras/stu349)
- Neyrinck, M. C. 2008, MNRAS, 386, 2101, doi: [10.1111/j.1365-2966.2008.13180.x](https://doi.org/10.1111/j.1365-2966.2008.13180.x)
- Park, C., Choi, Y.-Y., Vogeley, M. S., et al. 2007, ApJ, 658, 898, doi: [10.1086/511059](https://doi.org/10.1086/511059)
- Patiri, S. G., Prada, F., Holtzman, J., Klypin, A., & Betancort-Rijo, J. 2006, MNRAS, 372, 1710, doi: [10.1111/j.1365-2966.2006.10975.x](https://doi.org/10.1111/j.1365-2966.2006.10975.x)
- Peebles, P. J. E. 2001, ApJ, 557, 495, doi: [10.1086/322254](https://doi.org/10.1086/322254)
- Peper, M., & Roukema, B. F. 2021, MNRAS, 505, 1223, doi: [10.1093/mnras/stab1342](https://doi.org/10.1093/mnras/stab1342)
- Pisani, A., Sutter, P. M., Hamaus, N., et al. 2015, PhRvD, 92, 083531, doi: [10.1103/PhysRevD.92.083531](https://doi.org/10.1103/PhysRevD.92.083531)
- Rojas, R. R., Vogeley, M. S., Hoyle, F., & Brinkmann, J. 2004, ApJ, 617, 50, doi: [10.1086/425225](https://doi.org/10.1086/425225)
- . 2005, ApJ, 624, 571, doi: [10.1086/428476](https://doi.org/10.1086/428476)
- Sahlén, M. 2019, PhRvD, 99, 063525, doi: [10.1103/PhysRevD.99.063525](https://doi.org/10.1103/PhysRevD.99.063525)
- Sorrentino, G., Antonuccio-Delogu, V., & Rifatto, A. 2006, A&A, 460, 673, doi: [10.1051/0004-6361:20065789](https://doi.org/10.1051/0004-6361:20065789)
- Strauss, M. A., Weinberg, D. H., Lupton, R. H., et al. 2002, AJ, 124, 1810, doi: [10.1086/342343](https://doi.org/10.1086/342343)
- Sutter, P. M., Lavaux, G., Wandelt, B. D., & Weinberg, D. H. 2012a, ApJ, 761, 44, doi: [10.1088/0004-637X/761/1/44](https://doi.org/10.1088/0004-637X/761/1/44)
- . 2012b, ApJ, 761, 187, doi: [10.1088/0004-637X/761/2/187](https://doi.org/10.1088/0004-637X/761/2/187)
- Sutter, P. M., Pisani, A., Wandelt, B. D., & Weinberg, D. H. 2014, MNRAS, 443, 2983, doi: [10.1093/mnras/stu1392](https://doi.org/10.1093/mnras/stu1392)
- Sutter, P. M., Lavaux, G., Hamaus, N., et al. 2015, Astronomy and Computing, 9, 1, doi: [10.1016/j.ascom.2014.10.002](https://doi.org/10.1016/j.ascom.2014.10.002)
- Veyrat, D., Douglass, K. A., & BenZvi, S. 2023, ApJ, 958, 59, doi: [10.3847/1538-4357/acf4f5](https://doi.org/10.3847/1538-4357/acf4f5)
- von Benda-Beckmann, A. M., & Müller, V. 2008, MNRAS, 384, 1189, doi: [10.1111/j.1365-2966.2007.12789.x](https://doi.org/10.1111/j.1365-2966.2007.12789.x)
- Zhao, C., Chuang, C.-H., Kitaura, F.-S., et al. 2020, MNRAS, 491, 4554, doi: [10.1093/mnras/stz3339](https://doi.org/10.1093/mnras/stz3339)
- Zhao, C., Variu, A., He, M., et al. 2022, MNRAS, 511, 5492, doi: [10.1093/mnras/stac390](https://doi.org/10.1093/mnras/stac390)